

Modelling of Exploding Foil Initiator and Related Circuitry for Variable Mode of Operation.

A. J. Borman^a, C. F. Dowding^a and D. Seddon^b

^a*School of Engineering, University of Lincoln, Lincoln, United Kingdom, LN6 7TS;*

^b*Teledyne-e2v, 168 Sadler Road, Lincoln, United Kingdom, LN6 3RS*

* Corresponding Author

Telephone: +44 (0) 1522 837920

E-mail: aborman@lincoln.ac.uk

Received 28th November 2018; received in revised form 20th March 2019; accepted 25th March 2019

Alexander Borman is a lecturer at the University of Lincoln with a research interest in exploding foil initiator (EFI). Orcid ID: 0000-0002-6819-8653

Dr Colin Dowding is a senior lecturer at the University of Lincoln with research interests in application of lasers to energetic events, ultra-fast motion, micro-machining and polymer bonding.

Dick Seddon is a technical lead at Teledyne-e2v, working with Exploding Foil Initiators (EFI) and Electronic Safety and Arming Units (ESAU).

Modelling of Exploding Foil Initiator and Related Circuitry for Variable Mode of Operation.

Analytical and numerical models, validated against published data, were developed to calculate the velocity and time of arrival duration (ToAD) of the flyer-plasma material at the top of the barrel of an exploding foil initiator (EFI), as commonly used in explosive devices. Such tools will aid system designers in the optimization of capacitor discharge circuit (CDC) or EFI bridge material properties.

The analytical elements of the approach developed support the requirement for consideration of mass ejection variation with respect to initial capacitor voltage.

The numerical elements of the approach developed demonstrate that EFI design alteration to increase flyer mass is less effective in reducing ToAD than supply voltage modulation via the CDC. This finding is of particular relevance for in situ control of functional performance characteristics. This work goes on to demonstrate that such control is impracticable when using HNS, since the initial capacitor voltages necessary to yield appropriate ToAD for deflagration deliver insufficient energy to instigate a response from the EFI.

Keywords: exploding foil initiator; time of arrival duration; finite element modelling

1 Introduction

Exploding foil initiators (EFI) are laminar structured devices, first developed in the 1970's at Lawrence Livermore National Laboratory (1). Most prominently, the EFI is implemented as the first stage of a detonation train by discharging a high voltage capacitor through a thin, shaped foil "bridge" causing state changes from solid through to ionized plasma. This discharge is instigated by means of closing a triggered vacuum switch. An electrical insulator layer is located above the bridge layer and beneath a hole (barrel) in the layer above. A portion of the insulator layer is ejected up the barrel and into an explosive pellet positioned atop. Typical operation here initiates detonation

within the pellet, which may go on to initiate further detonations in the explosive train.

Schmidt et al. (2) consider modification of the Gurney equations to calculate velocities and positions of the flyer layer. The Gurney equations, are a set of equations which characterize the initial velocities of fragments emanating from bombs, shells or grenades (3). Schmidt et al. adapted these equations for EFI analysis, using an altered experimental power curve to act as the time dependent energy term in these equations. There is, however, a requirement in this method for empirical treatment of energy and power post-burst of the bridge and correction factors in order to produce good correlations. Whilst the Gurney equations produce good comparisons with experimental work (2), the Schmidt et al. model had not been validated when considering the variables of the materials and geometry of the flyer and foil.

Furnberg et al. also produced an empirical model describing the resistance of the bridge, which changes during firing of the EFI, containing multiple electrical parameters which are variable to optimize the correlation between the model and experimental data (4). The Furnberg et al. model simulates the electrical elements of the EFI's capacitor discharge circuit (CDC). The model was formed from two equations, the first describing the pre-burst period of the bridge, the second the post-burst period. Furnberg et al. note that, of the seven parameters featured in the pre-burst equation, six are determined through "trial and error" with previous experience governing which key parameters are taken into consideration (4). The model calculates accumulated energy and variation in resistance and feeds these values back into the firing system circuit model, denoting the burst energy as the point at which the modelling approach is switched from pre- to post-burst firing calculations. Extrapolation of the model to larger bridge sizes was conducted and successfully met experimental trial results (4).

Ghosh produced a simulation of an EFI, working on the assumption that the foil exhibits linear resistivity variation with temperature change and that energy

accumulation in the foil is equal to the amount of Ohmic heating (5). Changes in state are considered and the current density at the point of burst is used to calculate a flyer velocity, based on the Gurney equations. Based on a construction of copper foil and Mylar flyer, Ghosh's EFI flyer velocities were predicted to be between 1.4 and 2.4 km.s^{-1} . The model was then varied for configurations of different EFIs and compared with the results of other journal papers with variable results. Ghosh notes that a lack of information for some bridge materials limited the reliability of the simulation in some cases. The temperature response is also noted to be too simplistic when assumed to be purely linear, requiring a non-linear resistivity model. It was also noted that, as the time to burst increased, accuracy fell owing to the heat dissipation that had not been factored into the model (5). Ghosh concluded that this simplified model is only suitable for copper bridges with less than $1\mu\text{s}$ burst times (5).

Nappert modelled EFI operation by calculating bridge foil current as a function of time, feeding this into the Gurney equation to calculate flyer velocity based on the current density at the time of burst (6). Conservation of momentum equations combined with initiation criterion for specific explosives were then used to predict the effect of the EFI on the explosive pellet. Nappert notes that, whilst the high voltage predictions are in line with experimental results, lower voltage predictions are not as closely correlated with observed velocities (6). Additional work recommended by Nappert would be the collection of further data in order to fit capacitor discharge and bridge foil resistivity. It should be noted that Nappert's work utilized parameters for the Gurney equation calculated by other researchers (6).

Smetana et al. used finite element analysis (FEA) to model a thick film initiator, used as a safety device in the automotive industry. Smetana et al. noted the importance of the materials chosen for construction and their effect on the thermal conductivity of the device and the requirement for numerical simulation to both optimize the design of

the unit and characterize material diffusion occurring within it (7). It should be noted that the thick film initiator discussed in (7) differed in its layers of construction, hence, whilst similar methodologies may be applied here, results may differ.

Chritensen and Hrousis began to progress modelling of the EFI into three dimensions using magnetohydrodynamic simulation on a range of EFI sizes (8). These models considered both varying current and voltage in the system; model validation highlighted areas for further development, including future validation of global equations of state for bridge materials (8).

One such explosive that may be initiated by the EFI is hexanitrostilbene (HNS), detonated through shock by the impact of EFI flyer layer and vaporized bridge material (9). When considering HNS, Schwarz, (9) investigated the initiation of various grades and densities of this material using EFI. Schwarz's findings demonstrated that lower impact pressures reduced the probability of detonation and that longer pulse durations (achieved by increased thicknesses of the flyer layer) reduced impact pressure. Schwarz also demonstrated the non-linearity of the boundary between initiation and non-initiation whereby, as impact duration increases beyond $1.5\mu\text{s}$, the pressure required for initiation remains constant. Furthermore, grain size of the HNS was shown to influence the trends displayed in sensitivity; coarser textured explosives were demonstrated to be more sensitive to low pressure, longer duration impacts, whilst fine grain explosives exhibited more sensitivity at higher pressures (10). The shape of the interaction face of the shock-front has also been demonstrated to wield influence on initiation behaviour (11, 12). (12) also identifies the time at which the explosive acquires the maximum amount of energy from the initial shock to be of importance in critical energy calculations. This instant can be identified using time of arrival, from analytical calculation (Section 2.1) or via empirical measurement (13), in addition to ToAD.

Detonation has been shown to not be immediate upon impact of the flyer, the resulting compression waves through the explosive causing decomposition of the material which accelerates the wave front; should this exceed the material's threshold velocity for detonation (14), 7-7.1 km.s⁻¹ for HNS (15), the reaction has undergone the process of deflagration to detonation transition (DDT) (14) and the process of detonation takes over.

Flyer-explosive interaction has been observed to be of importance when considering system behavior, the work of (13) utilized an experimental technique to measure the velocity of ejected material from the barrel at high speed with the pellet removed, for a range of initial capacitor voltages. This work sought to understand the mode of operation of EFI in greater detail for the purpose of controlling and modifying this behavior in line for selective deflagration or detonation modes of operation.

Deflagration has been identified as achievable using EFI (16, 17).

From the observations and postulations presented within (13), analytical and numerical models have been developed and are presented herein and compared with the data of (13). The full experimental procedure has been presented previously, (13), and hence will not be reproduced here; however, where additional processing to the raw data collected has taken place, such processes will be described.

2 Model Development

Time of arrival duration (ToAD) has been predicted for an EFI driven by a CDC using a finite element model developed within a simulation package (Ansys 17.1, Explicit Dynamics) with initial boundary conditions calculated analytically. The model begins from initial electrical calculation, culminating in flyer velocity.

The electrical circuit considered is a closed loop RLC series circuit with closing of a triggered vacuum switch commencing circuit operation.

2.1 Preliminary Analytical Calculations

The analytical calculation steps described herein build upon the observations of (13) and can be broadly broken down into three phases: a time iterated phase determining the state of the bridge; an energy calculations phase which determines the transfer of the remaining energy from the capacitor and the solution phase reporting flyer ejection information (i.e. fire/no fire; velocity).

2.1.1 Time Iterated Phase

In the calculations which follow, t is the time the calculation has reached; if t is less than the activation time of the trigger vacuum switch, s , in the circuit, then

$$I_s = \frac{I_{max}}{s} t \quad (1)$$

where I_s is the current for that time step. Otherwise, if t is greater than or equal to s , I_s is calculated thus:

$$I_s = I_{max} \left(e^{\frac{-(t-s)}{RC} - \frac{R(t-s)}{L}} \right) \quad (2)$$

where R is the resistance, C is the capacitance and L is the inductance of the circuit.

Whilst resistance is variable during operation (see equation 3), for the purposes of this work, it is assumed to be fixed during each time step iterated.

2.1.2 Energy Calculation Phase

Basic circuit calculations (18), allow use of current to calculate the cumulative energy transferred during time t . This energy is then all assumed to be transferred to the EFI bridge (valid as long as the initiation duration is $< 1\mu s$, as described by Ghosh (5)) and cause temperature increase and a change of state within.

To identify the nature of the bridge during each time step, the energy required to raise temperatures in particular states of matter or transition between states is calculated

using standard calculations of internal energy and heating (18). For the purposes of this work, the percentage ionization of the bridge for initiation to occur was set to 20%, in line with other works (19). This based on the calculations of (20), considering first ionization energy of copper, predicted burst according the work of (21), predicted burst pressures and the Saha ionization equation (22).

The cumulative energy is compared with these energy requirements and hence the state of the bridge identified. If sufficient energy to initiate the flyer transition has been transferred, the calculation progresses to the next phase, otherwise the time iteration phase repeats, t increasing by a time step. The flyer is assumed to begin traversal of the barrel immediately upon 20% ionization being achieved.

If the calculation remains in phase two, resistance of the bridge is varied to reflect the current state of the bridge, standard equations (18) used for individual states of matter, accounting for changes in temperature and hence associated changes in resistance, with equations 3a-c used for transitory states between solid and liquid, liquid and gas and gas and plasma respectively.

$$R = \left(\frac{E_x - E_s}{E_m - E_s} \right) R_L + \left(1 - \left(\frac{E_x - E_s}{E_m - E_s} \right) \right) R_S \quad (3a)$$

$$R = \left(\frac{E_x - E_L}{E_v - E_L} \right) R_V + \left(1 - \left(\frac{E_x - E_L}{E_v - E_L} \right) \right) R_L \quad (3b)$$

$$R = \left(\frac{E_x - E_v}{E_I - E_v} \right) R_P + \left(1 - \left(\frac{E_x - E_v}{E_I - E_v} \right) \right) R_V \quad (3c)$$

Here E_x denotes the cumulative energy transferred, the subscripts s, m, l, v and p on the energies and resistances identifying solid, melting, liquid, vapor or plasma states.

2.1.3 Analytical Solution

If sufficient energy to reach 20% ionization has been transferred, then the time iterated phase is complete and phase three of the calculation commences. The cumulative energy transferred is compared with the total energy stored in the capacitor initially, calculated using standard capacitor equations (18). The EFI is deemed unable to draw

sufficient energy from the capacitor to fire if the model produces a difference less than or equal to zero. If the difference is greater than zero then all of the energy remaining in the capacitor is assumed to be transferred to the kinetic energy of the ejected material (i.e. bridge and flyer). This remaining energy, denoted E_K , is then substituted into the Gurney equation for an infinitely tamped structure (in line with the geometry of the EFI used to gather the empirical data used for verification). This is re-arranged to form equation 4.

$$v_f = \left(\frac{M}{C} + \frac{1}{3}\right)^{-\frac{1}{2}} \cdot \sqrt{2E_K} \quad (4)$$

where M is the mass of the flyer, C is the mass of the bridge and v_f is the ejected velocity of the flyer. As the bridge has smaller dimensions than the barrel, M was calculated based on empirical observations from (13). M is taken to be the area of the ejected bridge multiplied by the thickness and density of the flyer layer, in line with observations from other work (13).

A correlation between observed mass ejection and initial firing voltage was identified and extrapolated for firing voltages beyond the firing conditions of the EFI-CDC system.

2.2 Numerical Model

This velocity is then fed into the initial conditions of the numerical model to compute a ToAD; hence calculation from initial electrical conditions to ejected flyer velocity and ToAD is demonstrated. ToAD from these calculations is considered equivalent to the time at which an explosive has acquired its maximum amount of energy from initial shock interaction, identified by (12) to be key to calculating the critical energy criterion.

The model was computed for a range of initial capacitor voltages: 0 – 3000V. The model was also computed considering two mass boundary conditions: the mass of a

fixed volume (defined by initial bridge geometry, as has been considered in previous studies (6)) and a mass which varies with initial capacitor voltage (based on observations from (13)). The results from both of these scenarios are considered Section 4.

The geometry of the region of interest of the EFI (around the barrel) was modelled to include all layers: the tamper, the conductive bridge, the insulating flyer and the barrel with hole aligned axially with the bridge center. Model dimensions conformed with the manufacturing specification of the EFI used in the empirical investigation (13) and a plane of symmetry transecting the center of the barrel was applied to increase solving efficiency (see figure 1).

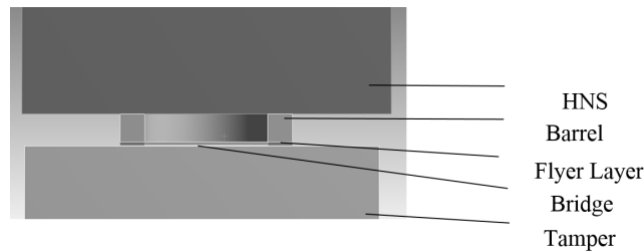


Figure 1. EFI cross section from FEA model.

The input variable for the numerical model was the flyer velocity, which has been demonstrated empirically to be dependent upon initial capacitor voltage. Calculation of the input velocity was predicted analytically for a range of initial capacitor voltages which were then applied to the underside of the bridge.

Once material defined strain limits (23) within individual mesh elements were exceeded, these elements were recorded by the model as having failed; however, their momentum was retained in the simulation. This is comparable with a flyer breaking apart during transition. Whilst thick flyers have been demonstrated to remain solid, thinner flyers have been shown to vaporize, ionize and breakup (24, 25). The expansion and traversal of flyer layer and the plasma that trailed it were modelled translating up the barrel.

Several distinctive events within the flyer transition of the barrel are predicted; figure 2 traces these kinematics of the top and bottom surfaces of the flyer (henceforth denoted ‘A’ and ‘B’, respectively) throughout their journeys up the barrel and into the underside of the pellet and identifies these events.

Prior to point 1, A is accelerated up the barrel. Between points 1 and 2 A has reached a constant velocity and, at point 2, begins to decelerate owing to impact with the pellet mounted at the top of the barrel. This impact is witnessed by the displacement trace of A provided in figure 2. The deceleration of A persists until point 3 as it continues to impact the explosive pellet. Points 3 to 4 exhibit the ongoing impact as trailing material (between A and B) compresses to cause re-acceleration of A.

Oscillations in B’s velocity and A’s displacement between points 4 and 5 demonstrate the re-compaction of the ejected material.

Figure 2 shows B arriving at the top of the barrel, denoted as a displacement of 1. The velocity of A also rapidly decelerates at point 5. As such, for the purposes of this work, impact is defined to have ended at point 5.

It should be noted that any shockwaves generated by energetic material impacted have been disregarded in this work to focus on variable mode of independent operation of the EFI unit.

The profile traced in Figure 2 does not contradict those detected via velocimetry methods (26). The velocity profile of the trailing face (B) is very different to that of the leading face (A). When using optical means to track such motion, the bulk nature of the material in transit would partially obscure the independent propagation of surfaces A and B up the barrel. Furthermore, velocimetric techniques (26, 27) with line-of-sight real-time velocity measurements, observing a flyer during barrel transit, will not see deceleration of A between points 2-3 as no material exists atop the barrel for interaction with A. Where windows are used to mimic a flyer-pellet impact event, traditional flyer

material such as kapton is transmissive at multiple wavelengths wherein copper bridge plasma will be emissive (28, 29); hence, surfaces A and B will be indistinguishable through velocimetry. The model presented herein allows users to investigate the critical interaction between ejected material and explosive pellet that would take place during real-world operation. Comparable results with acceleration periods of the same order of magnitude as previous studies are demonstrated (26).

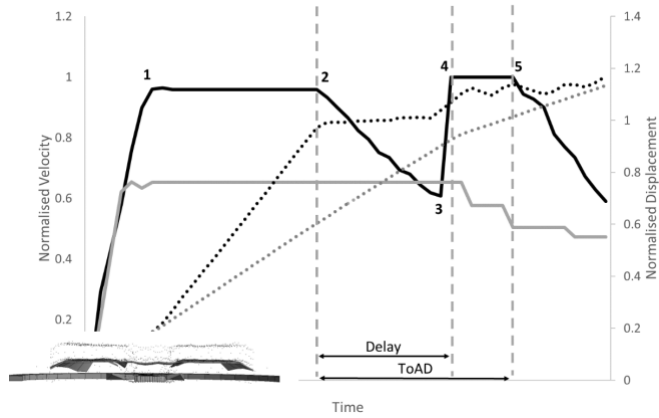


Figure 2. Normalised flyer velocity and displacement profile during barrel translation: leading face (A) velocity (—) and displacement (…), trailing face (B) velocity (—) and displacement (…). Inset: schematic cross section of EFI during initiation showing leading face (A) and trailing face (B) of the ejected material.

The simulation observed the time delay between flyer front (A) and end (B) of material arrival to vary with velocity. Simply described, higher velocity inputs resulted in the ejected material becoming proportionally more dense as it traversed the barrel. As a result, ToAD varied dependent upon initial conditions.

3 Laboratory Experimentation

In conjunction with the modelling, data collected from laboratory experimentation was also analyzed. The arrangement of (13), as displayed in figure 3, used two photodiodes to measure the time of initiation (PD1) and time of arrival (PD2) of material at the top of the barrel.

Additional to the processing of (13), a further point was identified from the signal detected at PD2, namely the time at which that signal returned to pre-event levels. The calculation method utilized was identical to that of (13), using discretization, looking for deviation from initial levels beyond user defined tolerances and marking this as the point of interest. The data was examined twice, once looking forward to identify the point where arrival of material began and the second looking in reverse to identify when the material finished arriving.

The difference between these two values can be calculated and hence a ToAD from the arrival of the flyer front and the end of the plasma traversing behind it can be discerned. Whilst mass ejected could not be directly measured in (13), estimates of volume of mass ejected were collated from micrographs for use in this work.

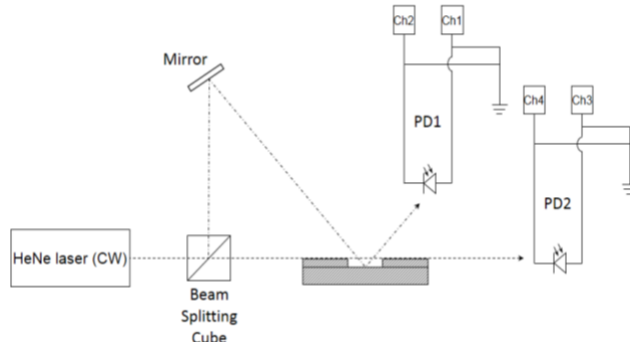


Figure 3. Laboratory experimentation setup.

4 Results and Discussion

Average velocities of flyer traversal along the barrel from the analytical model were recorded and compared with the laboratory results of (13) and are presented in figure 4.

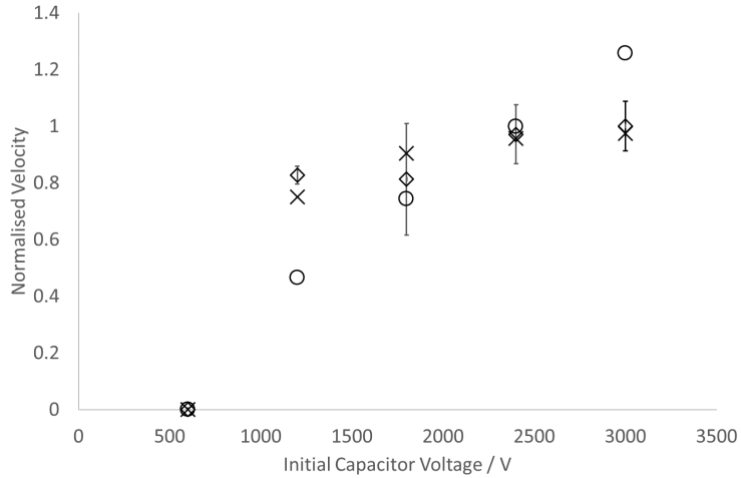


Figure 4. Laboratory measured (\diamond), with error bars, and analytically calculated flyer velocities, with fixed (○) and variable (X) mass of material ejected for a range of initial capacitor voltages.

The analytical calculations were performed twice for each initial capacitor voltage. The first data set assumed a constant mass of material ejected for each data point, as has been used by other authors (6). These points have a more linear trend than observed in the experimental results of (13). The initial capacitor voltage in figure 4, which displays three plots (fixed initial volume, capacitor voltage dependent volume and empirical measurement), indicates the voltage at which the two methods of mass ejection calculation intersect; this intersection marks the only point at which the fixed initial volume bridge geometry prediction of ejected mass is valid.

The second data series collected from the analytical model varied the mass removed by using measurements taken from micrographs from (13) to produce a relationship between initial voltage and ejected mass. The improved correlation in velocity trends highlights the validity of variable mass ejection with respect to initial capacitor voltage. A greater understanding of the relationship between initial capacitor voltages and mass ejected is required before a fully predictive analytical model can be developed for wider ranges of EFI.

As can be seen from figure 4, when considering a variable mass, the trend of the laboratory results is in close agreement to that of the simulated predictions for the initial

capacitor voltages trialed. As expected, lower initial capacitor voltages (meaning less energy stored within the capacitor) resulted in less energy transferred to the EFI and hence, less through the bridge, resulting in a lower flyer velocity. The strong agreement between laboratory experimentation and analytical modelling highlights the reliability of the findings identified by (13) of variable mass ejection for initial conditions, as well as the validity of the analytically predicted velocities.

From the numerical model ToAD were recorded for a range of velocities. These ToAD were compared with empirical results (13), as shown in figure 5. Here it can be seen that these model results correlate well and are of the same order of magnitude as results from other studies (6). Empirical data for lower flyer velocities were not obtained as, when considering figure 4, lower velocities require lower initial capacitor voltages. It has already been demonstrated both experimentally and, with this work, analytically, that these lower velocities are not achievable for the EFI model tested (the CDC energy is insufficient to vaporize the bridge).

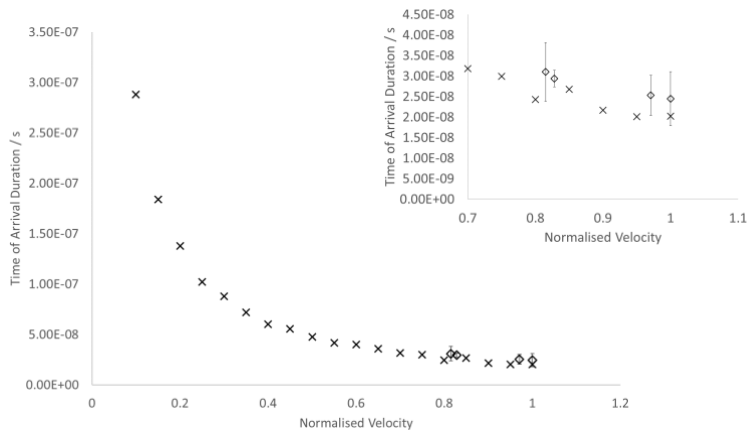


Figure 5. Laboratory measured (\diamond) and numerically modelled (X) Time of arrival duration (ToAD) for material ejected at a range of initial velocities. Inset: Magnification of right-hand region of graph.

ToAD was observed to be extended by the increased distance between the front (A) and rear (B) surfaces of the ejected material. Numerical modelling has demonstrated that lower velocities produced slower barrel transitions and a non-linear relationship between velocity and ToAD. Whilst increasing ToAD has been investigated previously

through the utilization of variable flyer thickness, as discussed earlier, this work demonstrates that some controllability through initial capacitor voltage is also possible.

The numerical model offers explanation for the temporal elongation of material ejection: during initiation the flyer layer domes due to flyer and bridge material expansion, facilitating elongation of the material to be ejected. The initial doming of the flyer whilst remaining attached is in line with (30); furthermore, bridge expansion aligns with (31). Comparison of results with other authors works highlights similarity in delay times between the model predictions of this work and those of (32) for the central region of the bridge and flyer. Behaviour predictions of this work differ from those of (32) in peripheral regions of the flyer and bridge. Bridge geometry within the FEA model of this work was simplified (by removal of complex curvature). The plume front (A) of arriving material demonstrably differed in shape as a result of bridge geometry modification. It is proposed that this is the reason for differing behaviour prediction concerning peripheral regions of the flyer and bridge between this study and that of (32). The advantage of the numerical model presented herein is its ability to solve without the requirement for supercomputer access (as with (32)), whilst still predicting comparable ToAD.

Increased time durations between points 2 and 4 were observed within the FEA model for lower initial capacitor voltages, denoting greater temporal separation between the top (A) and bottom (B) of material ejection plume, increasing the ToAD. Larger capacitor voltages/greater velocity flyers see a greatly reduced region 2-4 and hence shorter ToAD.

Use of numerical modelling to simulate voltage increase, for the purpose of influencing flyer velocity, highlights a reduced overall time between stages 2-5. The time in each phase of transit is increased; however, some phases of the transit are increased by a greater proportion. Reduction in voltage yields an increased time delay

between the leading (A) and trailing (B) edge. Higher voltages have shorter transit times without reaching a maximum velocity by the end of the barrel.

When considering the proportion of time in each phase of transit, reduction in voltage yields lower initial velocities but also reduces the proportion of the transition in stages 2-4 whilst increasing the proportional duration in stage 4-5. Whilst lower voltages produce a longer transit duration, more of the transit duration is spent in the final stage; delivering a lower momentum over a longer time duration. By considering the leading face (A), the time dependent delivery of momentum (and therefore force and pressure) to the pellet becomes attainable.

Other studies have looked at increasing mass through increased flyer thickness and its influence on velocity (33, 34, 35). Comparison between the signal modulation approach proposed herein and flyer mass increase is plotted in figure 6; mass increase reduces the overall proportion of transit in stages 2-4 and increases the duration of stage 2-4 as well as stage 4-5. The ToAD is defined as in figure 2; whilst the velocity profile is not typical of that observed, this is owing to the separation of leading and trailing surfaces, A and B respectively. These authors can find no evidence of independent velocity logging of surfaces A and B in literature.

Increasing mass exhibits a similar trend in transit profile modulation to that of reducing initial capacitor voltage although the proportional variation of velocities are not equal.

This highlights that either increasing the mass of flyer or reducing initial capacitor voltage increases the distance between front (A) and trailing (B) edge of ejected material. Furthermore, figure 6 demonstrates that, whilst mass modification does influence ToAD, a halving of initial velocity through voltage modulation has greater proportional impact on the ToAD compared with doubling the mass, particularly during the 2-4 phase.

Mass modification is clearly impracticable following initiator installation and cannot be implemented remotely prior to EFI operation from a single installed EFI unit. Despite the apparent functional benefits of voltage modulation, it is known that the delivery of energy required to potentially yield deflagration effects (16) is not obtainable from the EFI-CDC in standard operation.

EFI initiations where stage 4-5 is not present (i.e. high initial capacitor voltage or low mass flyers) do not reach their maximum velocity after stage 3 because they are still accelerating at the top of the barrel. In these cases, the flyer does not carry its maximum possible momentum as it meets the bottom of the pellet. This suggests that operating this geometry of EFI in combination with the length of barrel implemented in (13) whilst using a high initial capacitor voltage is inefficient.

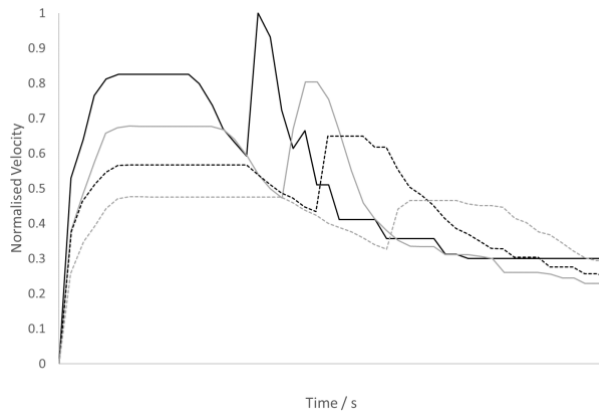


Figure 6. Numerical model flyer velocity profile of upper surface (A) during barrel transition: control example (—); double the flyer mass (···); half the initial capacitor voltage (—); half the capacitor voltage and double the mass (···).

5 Conclusion

The work presented involves analytical and numerical models which, in combination, enable calculation of the velocity of both the top and bottom surface of EFI ejected flyer-plasma material. By extension, such velocity trends can infer the time dependent delivery of momentum (and therefore force and pressure) to the pellet. These velocities also facilitate the prediction of the time of arrival duration (ToAD) of the ejected

material at the bottom surface of an explosive pellet for which impact duration is of particular relevance.

Both the numerical model and its analytical initial conditions have independently produced results which are validated by the data collected in other studies. Furthermore, the variable mass ejection observed previously has been supported by comparison of its inclusion and exclusion from the analytical calculation; inclusion of a variable mass demonstrated a much closer correlation with data collected experimentally. This, combined with the demonstrable influence of mass on the final ToAD profile, highlights an area of further investigation necessary for the construction of an holistic model incorporating fully predictive mass variability based on input parameters such as initial capacitor voltage.

A numerical model compared the influence of flyer mass variation to that of voltage modulation on the flyer velocity and therefore ToAD. Whilst both influence the final ToAD profile, mass variation was observed to have a smaller effect than that of voltage modulation and is functionally impracticable without hardware modification. Conversely, voltage modulation is inherently variable and therefore well suited to remote and/or short notice implementation to enable selectable modes of EFI operation.

The simulation work presented herein demonstrates that the reduction of ToAD, suitable to achieve a non-detonation effect such as deflagration, with the present capacitor discharge circuit (CDC) and commercial EFI configuration is not viable. Whilst this work shows that lower initial velocities can yield increased ToAD, these may not be physically reproducible. This is because the capacitor voltages required to initiate a flyer transition of such a low velocity are insufficient to vaporise the bridge. To achieve switchable modes of operation from a single piece of EFI hardware, a design modification to either the EFI or the CDC is deemed to be necessary as a result of this work.

References

- (1) Stroud, J. R., "A New Kind Of Detonator - The Slapper," Lawrence Livermore National Laboratory, Livermore, 1976.
- (2) Schmidt, S. C., Seitz, W. L., and Wackerle, J., "An Empirical Model to Compute the Velocity Histories of Flyers Driven by Electrically Exploding Foils," Los Alamos Scientific Laboratory, Los Alamos, New Mexico, 1977.
- (3) Gurney, R. W., "The Initial Velocities of Fragments from Bombs, Shells, Grenades," Ballistic Research Laboratories, Aberdeen, Maryland, 1943.
- (4) Furnberg, C. M., Peevy, G. R., Brigham, W. P. and Lyons, G. R., "Computer Modelling of Electrical Performance of Detonators," in 31st Joint Propulsion Conference and Exhibit., San Diego, 1995.
- (5) Ghosh, A., "Modelling and Simulation of Burst Phenomenon in Electrically Exploded Foils," Terminal Ballistics Research Laboratory Electro Explosive Devices (EED) Division, Ropar, India, 2012.
- (6) Nappert, L., "An Exploding Foil Initiator System," Defence Research Establishment, Valcartier, Québec, 1996.
- (7) Smetana, W., Reicher, R., and Homolka, H., "Improving reliability of thick film initiators for automotive applications based on FE-analyses," Microelectronics Reliability, vol. 45, pp. 1194 - 1201, 2005.
- (8) Christensen, J. S., and Hrousis, C. A., "Three-Dimensional Magnetohydrodynamic Simulation of Slapper Initiation Systems," in 14th International Detonation Symposium, Coeur d'Alene, ID, 2010.
- (9) Schwarz, A. C., "Shock-Initiation Sensitivity of Hexanitrostilbene (HNS)," in Seventh Symposium (International) on Detonation, 1981.
- (10) Price, D., "Effect of Particle Size on the Shock Sensitivity of Pure Porous HE," Naval Surface Weapons Centre, Silver Spring, Maryland, 1986.
- (11) James, H. R., and Hewitt, D. B., "Critical Energy Criterion for the Initiation of Explosives by Spherical Projectiles," Propellants, Explosives, Pyrotechnics, vol. 14, no. 6, pp. 223 - 233, 1989.
- (12) James, H. R., "Critical Energy Criterion for the Shock Initiation of Explosives by Projectile Impact," Propellants, Explosives, Pyrotechnics, vol. 13, no. 2, pp. 35 - 41, 1988.
- (13) Borman, A. J., Dowding, C. F., Griffiths, J. D., and Seddon, D., "Exploding Foil Initiator (EFI) Modes of Operation Determined Using

- Down-Barrel Flyer Layer Velocity Measurement," Propellants, Explosives, Pyrotechnics, vol. 42, no. 3, pp. 318-328, 2016.
- (14) Brundage, A. L., "Modeling Compressive Reaction in Shock-Driven Secondary Granular Explosives," in ASME/JSM 2011 8th Thermal Engineering Joint Conference, Honolulu, Hawaii, 2011.
- (15) Eurelco, "HEXANITROSTILBENE (HNS)," July 2013. [Online]. Available: <http://www.eurelco.com/wp-content/uploads/2013/07/HNS.pdf>. [Accessed 14 July 2017].
- (16) Lienau, J. A., "Exploding Foil Initiator Qualifications," U.S. Army Missile Command, Redstone Arsenal, Alabama, 1993.
- (17) Graswald, M., "Precise Target Effects through Scalable Warhead Effects," in Delivering Precision Effects in a Complex Environment, Paris, 2013.
- (18) Pople, S., Advanced Physics, Oxford: Oxford University Press, 1996.
- (19) Yilmaz, M. Y., Design and Analysis of a High Voltage Exploding Foil Initiator for Missile Systems, Ankara: Middle East Technical University, 2013.
- (20) Richardson, D. D., Northeast, E. D., and Ryan, P. F., "An Exploding Foil Flying Plate Generator," Materials Research Laboratory, Melbourne, 1987.
- (21) Zentler, J. M., "FUSEL A Simple Simulation Model for a Flyer-Plate Detonator System," Lawrence Livermore National Laboratory, Livermore, 1982.
- (22) Chen, F. C., Introduction to Plasma Physics, New York: Plenum Press, 1977.
- (23) DuPont, "DuPont Products and Services: Polyimide Films," [Online]. Available: <http://www.dupont.com/content/dam/dupont/products-and-services/membranes-and-films/polyimde-films/documents/DEC-Kapton-HN-datasheet.pdf>. [Accessed 23 11 2018].
- (24) Bowden, M., PhD Thesis: The Development of a Laser Detonator System, Bedford: Cranfield University, 2014.
- (25) Zeng, Q., Li, B., Li, M., and Wu, X., "A Miniature Device for Shock Initiation of Hexanitrostilbene by High-Speed Flyer," Propellants, Explosives, Pyrotechnics, vol. 41, pp. 864-869, 2016.
- (26) Scholtes, J. H. G., Prins, W. C., Bouma, R. H. B., and Meulen, B., "Development of exploding foil initiators for future IM," in 2007 In-sensitive Munitions & Energetic Materials Technology Symposium

(IMEMTS): "New Programs, New Policies, New Strategies leading to New Joint Solutions", Miami, Florida, USA, 2007.

- (27) Xu, C., Zhu, P., Chen, K., Zhang, W., Shen, R., and Ye, Y., "A Highly Integrated Conjoined Single Shot Switch and Exploding Foil Initiator Chip Based on MEMS Technology," IEEE Electron Device Letters, vol. 38, no. 11, pp. 1610 - 1613, 2017.
- (28) Virk, H. S., Chandi, P. S., and Srivastava, A. K., "Physical and chemical response of 70 MeV carbon ion irradiated Kapton-H polymer," Bulletin of Materials Science, vol. 24, no. 5, pp. 529 - 534, 2002.
- (29) Ross, C. B., "Wavelengths and Energy Levels of Singly Ionized Copper Cu II LA - 4498," Los Alamos Scientific Lab., N. Mex., 1970.
- (30) Willey, T. M., Champliey, K., Hodgin, R., Lauderbach, L., Bagge-Hansen, M., May, C., Sanchez, N., Jensen, B. J., Iverson, A., and van Buuren, T., "X-ray Imaging and 3D reconstruction of In-Flight Exploding Foil Initiator Flyers," Journal of Applied Physics, vol. 119, no. 23, 2015.
- (31) Neal, W., and Bowden, M., "High Fidelity Studies of Exploding Foil Initiator Bridges, Part 2: Experimental Results," in AIP Conference Proceedings, Terchova, Slovakia, 2017.
- (32) Neal, W., and Garasi, C., "High fidelity studies of exploding foil initiator bridges, Part 3: ALEGRA MHD simulations," in AIP Conference Proceedings, 2017.
- (33) Waschl, J. A., and Hatt, D. J., "Characterization of a Small-Scale Exploding Bridge Foil Flyer Generator," International Journal of Impact Engineering , vol. 14, pp. 785 - 796, 1993.
- (34) Scholtes, G., and Prinse, W., "Development of Exploding Foil Initiators and Micro Chip EFIs," in 42nd Gun and Missile System Conference and Exhibition, Charlotte N.C., 2007.
- (35) Prinse, W. C., van t'Hof, P. G., Cheng, L. K., and Scholtes, J. H., "High Speed velocity measurements of an EFI-system," in Proceedings of the 27th International Congress on High-Speed Photography and Photonics, 2007.